

## The Atomic Interfacial Structure between $\alpha_2$ and $\gamma$ Phases within a TiAl Alloy in Lamellar Form

Fang Liu<sup>1</sup>, Guo-zhen Zhu<sup>1</sup>

<sup>1</sup>. State Key Laboratory of Metal Matrix Composites, School of Materials Science and Engineering, Shanghai Jiao Tong University, Shanghai, 200240, P. R. China.

Due to the attractive properties such as high strength-to-weight ratio and excellent high temperature creep and oxidation resistance, TiAl-based alloys with fully lamellar microstructure have been widely applied in producing aerospace and car engines [1-3]. The distribution of  $\alpha_2$  and  $\gamma$  phases, strongly affected by their interface, plays an important role in determining their mechanical properties at high temperature [4-6]. Although many researchers have investigated it by transmission electron microscopy [4, 7], the atomic interfacial arrangement and the chemical bonding nature have not been fully clarified. Therefore, we aim on analysing of the detailed interfacial structure in TiAl alloys.

We studied TiAl-based alloys synthesized by arc melting (at China Iron and Steel Research Institute Group). The lamellar structure was achieved by the heat treatment including 1340 °C for 0.5 h, 1 h and 2 h followed by air cooling. The microstructure morphology was studied by the optical microscopy and scanning electron microscopy. The samples were mechanically polished and etched by the aqueous reagent of 2% hydrofluoric acid and 10% hydrogen nitrate prior to the optical characterization. The TEM samples were prepared by the twin-jet electro-polishing technique with an electrolyte of 4% perchloric acid. The detailed atomic structure was investigated using a JEOL ARM200F Scanning Transmission Electron Microscopy (STEM) with a probe corrector.

The lamellar structure, consisting of  $\alpha_2$  (Ti<sub>3</sub>Al, DO<sub>19</sub>) and  $\gamma$  (TiAl, L1<sub>0</sub>) phases, was successfully synthesized through the above approaches. The lamellar spacing increases with increasing annealing time. A well-defined orientation relationship of  $\{111\}_\gamma // (0001)_{\alpha_2}$  &  $\langle 1-10 \rangle_\gamma // \langle 11-20 \rangle_{\alpha_2}$  was additionally confirmed using the selected area diffraction (SAD) technique (see Figure 1). There are always three sets of diffraction patterns co-existing within the same regions. The diffraction labeled by the yellow rectangle in figure 1 is from  $\alpha_2$  phase. The other two diffraction patterns, indicated by the red and green rectangles, belong to  $\langle 011 \rangle_\gamma$  and  $\langle 1-10 \rangle_\gamma$ , respectively. The atomic arrangement of  $\gamma$  phase viewed along  $\langle 011 \rangle_\gamma$  and  $\langle 1-10 \rangle_\gamma$  is different (see the STEM-high-angle annular dark-field (HAADF) images in figure 2 (b) and (c)) due to the ordered L1<sub>0</sub> structure with a slightly larger c axis. Although the c axis is not equivalent to the other two axes in  $\gamma$  structure, the c/a ratio is only in the range of 1.01-1.03 depending on the Al content. As shown in the STEM-HAADF images in figure 2,  $\alpha_2$  phase has brighter Z-contrast compared to the  $\gamma$  phase. Viewed from  $\langle 11-20 \rangle_{\alpha_2}$ , the Ti column has slight brighter contrast compared to the Ti-Al column. The interface between  $\alpha_2$  and  $\gamma$  phase is atomic sharp, as shown in figure 2 (d) and (e). In addition, we always detected the twinning (figure 2 (e)) and pseudo-twinning (figure 2(f)) of  $\gamma$  phase viewed along  $\langle 011 \rangle_\gamma$ . The pseudo-twinning refers as the mirror structure of  $\gamma$  phase forming at sides of  $\alpha_2$  phase with a dimension of ~2 nm.

The detailed atomic arrangement of the  $\alpha_2/\gamma$  interface is currently under investigated by atomic resolution STEM and electron energy-loss spectroscopy techniques (EELS). Different atomic models can be built to study their interface energy by applied first principles computation.

## References:

- [1] E. A. Marquis, J. M. Hyde, *Materials Science and Engineering R: Reports* 69 (2010) p. 37-62.  
 [2] E. A. Loria, *Intermetallics* 8 (2000), p. 1339-1345.  
 [3] H. Clemens, H. Kestler, *Advanced Engineering Materials* 2 (2000), p. 551-570.  
 [4] G. J. Mahon, J. M. Howe, *Metallurgical Transactions A* 21 (1990), p. 1655-1662.  
 [5] F. Appel, M. Oehring, R. Wagner, *Intermetallics* 8 (2000), p. 1283-1312.  
 [6] L. M. Hsiung, A.J. Schwartz, T. G. Nieh, *Scripta Materialia* 36 (1997), p. 1077-1022.  
 [7] L. Zhao, K. Tangri, *Philosophical Magazine A* 64 (1991), p. 361-386.  
 [8] Thanks for the supplying samples from China Iron and Steel Research Institute Group. We also thank Prof. Ji Zhang for helping and benefit discussions.

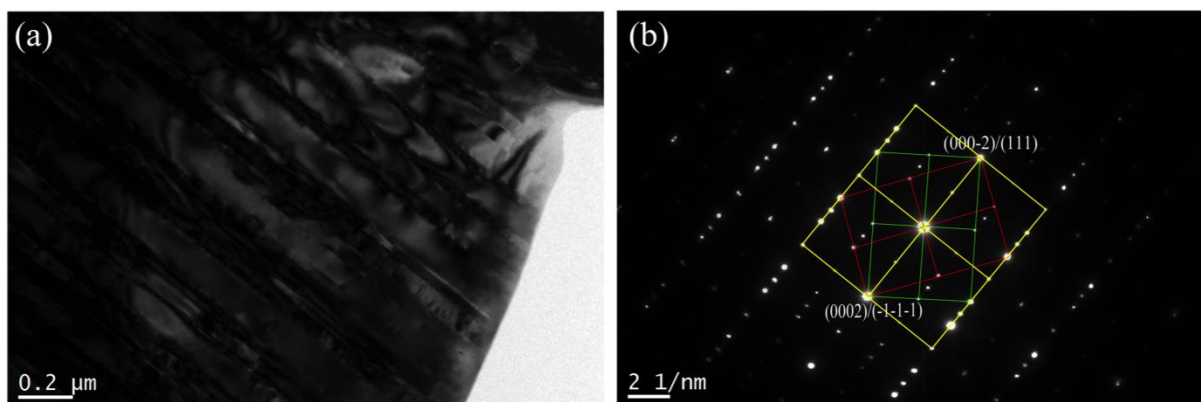


**Figure 1.** The lamellar structure. (a) the bright field image (b) the corresponding diffraction pattern.

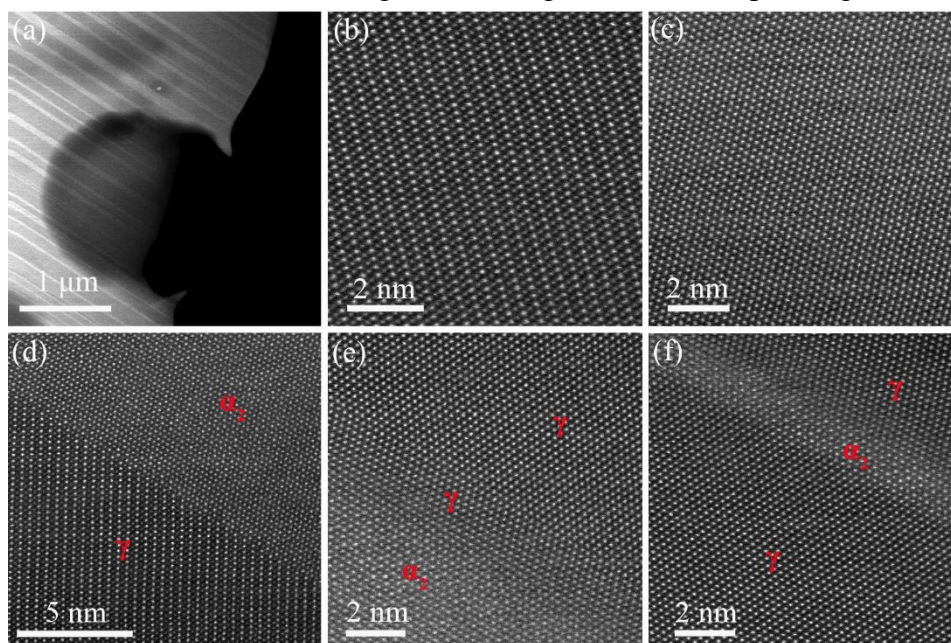


**Figure 2.** The atomic structure of lamellar microstructure. (a) the low magnification HAADF image (b)-(c) shows the atomic structure of  $\gamma$  phase when the beam is parallel to  $\langle 1-10 \rangle_\gamma$  and  $\langle 011 \rangle_\gamma$ , respectively (d) the interface of  $\gamma$  and  $\alpha_2$  (e)-(f) the twinning and pseudo-twinning, respectively.